



# Unchanged pulmonary toxicity of ZnO nanoparticles formulated in a liquid matrix for glass coating

Anne Thoustrup Saber, Niels Hadrup, Andrew Williams, Alicja Mortensen, Jozef Szarek, Zdenka Kyjovska, Alexander Kurz, Nicklas Raun Jacobsen, Håkan Wallin, Sabina Halappanavar & Ulla Vogel

To cite this article: Anne Thoustrup Saber, Niels Hadrup, Andrew Williams, Alicja Mortensen, Jozef Szarek, Zdenka Kyjovska, Alexander Kurz, Nicklas Raun Jacobsen, Håkan Wallin, Sabina Halappanavar & Ulla Vogel (2022) Unchanged pulmonary toxicity of ZnO nanoparticles formulated in a liquid matrix for glass coating, *Nanotoxicology*, 16:6-8, 812-827, DOI: [10.1080/17435390.2022.2152751](https://doi.org/10.1080/17435390.2022.2152751)

To link to this article: <https://doi.org/10.1080/17435390.2022.2152751>



© 2022 The Author(s). Published by Informa UK Limited, trading as Taylor & Francis Group.



[View supplementary material](#)



Published online: 08 Dec 2022.



[Submit your article to this journal](#)



Article views: 863



[View related articles](#)



[View Crossmark data](#)

## Unchanged pulmonary toxicity of ZnO nanoparticles formulated in a liquid matrix for glass coating

Anne Thoustrup Saber<sup>a,\*</sup>, Niels Hadrup<sup>a,b,\*</sup> , Andrew Williams<sup>c</sup>, Alicja Mortensen<sup>a</sup>, Jozef Szarek<sup>d</sup>, Zdenka Kyjovska<sup>a</sup>, Alexander Kurz<sup>e</sup>, Nicklas Raun Jacobsen<sup>a</sup> , Håkan Wallin<sup>f</sup> , Sabina Halappanavar<sup>c</sup> and Ulla Vogel<sup>a,g</sup> 

<sup>a</sup>National Research Centre for the Working Environment (NFA), Copenhagen, Denmark; <sup>b</sup>Division of Diet, Disease Prevention and Toxicology, National Food Institute, Technical University of Denmark, Copenhagen, Denmark; <sup>c</sup>Environmental Health Science and Research Bureau, Health Canada, Ottawa, Canada; <sup>d</sup>Department of Pathophysiology, Forensic Veterinary Medicine and Administration, University of Warmia and Mazury in Olsztyn, Olsztyn, Poland; <sup>e</sup>Techniplas NAG GmbH, Göttelborn, Germany; <sup>f</sup>National Institute of Occupational Health, Oslo, Norway; <sup>g</sup>DTU Food, Technical University of Denmark, Lyngby, Denmark

### ABSTRACT

The inclusion of nanoparticles can increase the quality of certain products. One application is the inclusion of Zinc oxide (ZnO) nanoparticles in a glass coating matrix to produce a UV-absorbing coating for glass sheets. Yet, the question is whether the inclusion of ZnO in the matrix induces toxicity at low exposure levels. To test this, mice were given single intratracheal instillation of 1) ZnO powder (ZnO), 2) ZnO in a glass matrix coating in its liquid phase (ZnO-Matrix), and 3) the matrix with no ZnO (Matrix). Doses of ZnO were 0.23, 0.67, and 2 µg ZnO/mouse. ZnO Matrix doses had equal amounts of ZnO, while Matrix was adjusted to have an equal volume of matrix as ZnO Matrix. Post-exposure periods were 1, 3, or 28 d. Endpoints were pulmonary inflammation as bronchoalveolar lavage (BAL) fluid cellularity, genotoxicity in lung and liver, measured by comet assay, histopathology of lung and liver, and global gene expression in lung using microarrays. Neutrophil numbers were increased to a similar extent with ZnO and ZnO-Matrix at 1 and 3 d. Only weak genotoxicity without dose-response effects was observed in the lung. Lung histology showed an earlier onset of inflammation in material-exposed groups as compared to controls. Microarray analysis showed a stronger response in terms of the number of differentially regulated genes in ZnO-Matrix exposed mice as compared to Matrix only. Activated canonical pathways included inflammatory and cardiovascular ones. In conclusion, the pulmonary toxicity of ZnO was not changed by formulation in a liquid matrix for glass coating.

### ARTICLE HISTORY

Received 9 September 2022  
Revised 22 November 2022  
Accepted 23 November 2022

### KEYWORDS

Zinc oxide; comet assay; genotoxicity; advanced materials; gene expression

## Introduction

Zinc oxide (ZnO) nanoparticles are widely used in the industry due to their technological qualities. One example is the addition of ZnO nanoparticles to glass surface coatings to provide UV blocking or anti-bacterial properties (Luther and Zweck 2013). There is evidence that occupational exposure to ZnO nanoparticles does occur (Ogura, Sakurai, and Gamo 2011; Cooper et al. 2017). Occupational exposure to ZnO nanoparticles during their manufacture and use may pose a potential health hazard (Hadrup et al. 2021b). The main potential exposure

pathways are dermal and pulmonary exposure, with the latter being of special interest in relation to handling powders during manufacture, as these can become airborne and be inhaled. Likewise, aerosols can be inhaled if the final surface coating product is sprayed on the intended surface. Data on the toxicity of ZnO composites are scarce and to the best of our knowledge, no *in vivo* pulmonary studies on the toxicity of ZnO surface coatings have been published.

In contrast, more information is available on the pulmonary toxicity of ZnO nanoparticles that are not sequestered in surface coatings: Inhalation of

**CONTACT** Anne Thoustrup Saber  [ats@nfa.dk](mailto:ats@nfa.dk)  National Research Centre for the Working Environment, Lersø Parkallé 105, DK-2100 Copenhagen Ø, Denmark

 Supplemental data for this article can be accessed online at <https://doi.org/10.1080/17435390.2022.2152751>

\*These authors contributed equally to this work.

© 2022 The Author(s). Published by Informa UK Limited, trading as Taylor & Francis Group.

This is an Open Access article distributed under the terms of the Creative Commons Attribution-NonCommercial-NoDerivatives License (<http://creativecommons.org/licenses/by-nc-nd/4.0/>), which permits non-commercial re-use, distribution, and reproduction in any medium, provided the original work is properly cited, and is not altered, transformed, or built upon in any way.

ZnO nanoparticles, in human volunteers, induces dose-dependent increases in neutrophil cell numbers in blood at 1 and 2 mg/m<sup>3</sup> for 4 h, increased blood levels of SAA at 1 and 2 mg/m<sup>3</sup>, and increased CRP at 0.5 mg/m<sup>3</sup>. It is important to note that these effects were observed at doses that are below the occupational exposure limits for ZnO in many countries (Monsé et al. 2018; Vogel and Cassee 2018). In another study, acute exposure of healthy human adults to 0.5 mg/m<sup>3</sup> mass concentration of ZnO (<0.1 µm in diameter) for 2 h did not induce acute-phase or pro-inflammatory reactions (Beckett et al. 2005). Zinc, among other metals, is a constituent of welding fumes, and ZnO and other welding fume substances can induce metal fume fever, characterized by flu-like symptoms (Greenberg and Vearrier 2015). Several rodent inhalation studies have reported pulmonary inflammation following exposure to ZnO nanoparticles. The pulmonary inflammation in the form of increased neutrophil numbers in BAL fluid gave no-observed-adverse-effect concentrations (NOAECs) in the range of 0.4–7 mg/m<sup>3</sup> (Ho et al. 2011; Adamcakova-Dodd et al. 2014; Chuang et al. 2014; Chen et al. 2015; Jacobsen et al. 2015; Larsen et al. 2016), and elevated acute phase response (Jacobsen et al. 2015; Hadrup et al. 2019).

The data on the genotoxic potential of ZnO are scarce and inconsistent. Elevated oxidative damage measured by 8-oxo-2'-dG was seen in rats after ZnO nanoparticle inhalation of 3.7 mg/m<sup>3</sup> (35 nm particle) and 45 mg/m<sup>3</sup> (250 nm) for 6 h (Ho et al. 2011). In addition, 8-oxo-2'-dG levels were increased in rats after intratracheal instillation of a high dose (33 mg/kg bw) of 50 nm ZnO nanoparticles (Chuang et al. 2014). On the contrary, Larsen et al. found no DNA damages assessed by the comet assay in mice after 1 h of inhalation of 58 (13 nm particle) or 53 mg/m<sup>3</sup> (36 nm) ZnO nanoparticle (Larsen et al. 2016) and a weak evidence of genotoxicity was noted in mice intratracheal instilled with ZnO nanoparticles (Hadrup et al. 2019).

As reviewed previously, the ZnO-mediated toxicity has been attributed to their dissolution leading to release of Zn<sup>2+</sup> ions. A recent study involving controlled exposure of healthy human volunteers to micro- and nano-sized ZnO, reported that the micro- and nano-sized ZnO induced similar acute phase response at the same deposited dose by

mass, whereas the deposited surface area did not predict acute phase response (Monsé et al. 2021).

Taking these data together, the pulmonary toxicity of ZnO in its pristine form is well described. However, to our knowledge, information on the toxicity of ZnO nanoparticles when inserted into a matrix is lacking. Our aim was to assess if the toxicity of ZnO nanoparticles was modified when present in a liquid binder matrix with organic compounds used for dip coating of glass. Our H<sub>0</sub> hypothesis was that ZnO nanoparticles formulated in the liquid matrix for glass coating had the same toxicity as pristine ZnO nanoparticles. The alternative, H<sub>1</sub> hypothesis, was the toxicity of ZnO formulated in a liquid matrix for glass coating had higher toxicity than the pristine ZnO nanoparticles. To test this, we exposed mice to 1) ZnO powder (abbreviated ZnO); 2) ZnO in a liquid matrix for glass coating (ZnO-Matrix); or 3) matrix alone (Matrix), *via* single intratracheal instillation. Pulmonary inflammatory response was assessed by changes in the cellular composition of bronchoalveolar lavage (BAL) fluid and by lung microscopy. Liver response to pulmonary injury was assessed by microscopy and genotoxicity in lung and liver was assessed by comet assay. In addition, changes in global gene expression in lung tissue using microarrays were also assessed to understand if and how formulation of ZnO in a liquid matrix influences the potential of ZnO to induce toxicity.

## Methods

### Test materials

The materials were supplied by Nanogate (Quierschied-Göttelborn, Germany). The materials were: 1) the ZnO powder Zincox<sup>TM</sup>10, also known as NRCWE-031 (here abbreviated ZnO); 2) ZnO in a glass matrix containing approximately 5 wt% ZnO (main solvent ethanol) (Pro.Glass Barrier 401 from Nanogate AG, partner in NanoSustain), also known as NRCWE-029 (here abbreviated ZnO-Matrix); and 3) the matrix with no ZnO with the same constituents as Pro.Glass Barrier 401 but without ZnO, also known as NRCWE-039 (here abbreviated Matrix). The two glass matrices (with and without ZnO) were tested in a liquid form. Under a non-disclosure agreement with the supplier (Nanogate), we

performed no physico-chemical characterization of 'pro. Glass barrier 401 without ZnO'. A TEM image of Zincox™10 can be seen in (Shi et al. 2012).

### **Preparation of particle suspensions**

The nanoparticles were suspended using the ENPRA protocol (Jensen and Kembouche 2014) in 0.2 mm filtered,  $\gamma$ -irradiated Nanopure Diamond UV water (Pyrogens: < 0.001 EU/mL, total organic carbon: < 3.0 ppb) containing 2% v/v serum from mice of the same strain (Hadrup et al. 2017). The suspensions were sonicated continuously for 16 min on an ice-waterbath using a Branson Sonifier S-450D (Branson Ultrasonics Corp., Danbury, CT) equipped with a 13 nm disruptor horn (Model number: 101-147-037, Branson Ultrasonics Corp., Danbury, CT). The amplitude was 10%. The particle mass concentration was 3.24 mg ZnO/mL for the two ZnO-containing suspensions (NRCWE-031 and NRCWE-029) corresponding to 162  $\mu$ g/mouse in a 50  $\mu$ L instillation volume. The NRCWE-039 without ZnO was prepared similarly to NRCWE-029 to be able to compare the effect of the dispersion liquid. The stock suspensions were further diluted in 2% v/v serum followed by 2 min of sonication, to provide lower dose levels.

### **DLS and zeta-potential characterization of particle suspensions**

The hydrodynamic size distribution and Zeta-potential of the nanoparticle dispersions were measured at three doses by Dynamic Light Scattering (DLS) using a Malvern Zetasizer Nano ZS (Malvern Instruments, Malvern, UK), at 25 °C. Data analysis was conducted in the Dispersion Technology Software version 7.11 (Malvern Instruments, Malvern, UK). Refractive and absorption indices as well as standard optical and viscosity properties were those for water. The refractive ( $R_i$ ) and absorption indices ( $R_s$ ) were set to 2.5 and 0.3, respectively.

### **Selection of doses**

Based on pilot data with the ZnO nanoparticle showing overt toxicity at 6 and 18  $\mu$ g/mouse (Jacobsen et al. 2015), doses of 2  $\mu$ g/mouse and below were selected. The instilled single doses of

ZnO were 0.22 (low), 0.67 (medium), and 2  $\mu$ g/mouse (high). ZnO Matrix doses had equal amounts of ZnO, while Matrix was adjusted to have an equal volume of matrix to ZnO Matrix. The Matrix contained only 5% of ZnO. The doses of Matrix were the same as ZnO-Matrix. Carbon black Printex 90 nanoparticles (162  $\mu$ g/mouse) were included as a benchmark positive control. Instillation of the single dose with 50  $\mu$ L of particle suspension was done as described previously (Jackson et al. 2011; Saber et al. 2012a; Hadrup et al. 2017). Control animals were instilled with sonicated vehicle.

### **Animal procedures**

The study was in compliance with the EC Directive 86/609/EEC and Danish law regulating experiments with animals (The Danish Ministry of Justice, Animal Experiments Inspectorate permission 2012-15-2934-00223). Seven-week old, female C57BL/6J BomTac mice (84 in total) were housed 2–6 per cage. Cages were made of polypropylene. Pinewood sawdust bedding and sticks of aspen wood and rodent tunnels served as enrichment (Brogaard, Skive, Denmark). Room temperature and humidity were  $21 \pm 1$  °C and  $50 \pm 20\%$ , respectively. Light was on from 06:00 a.m. to 6 p.m. The animals had *ad libitum* access to drinking water (tap water) and feed (Altromin no. 1324, Altromin International, Lage, Germany). The animals were allowed to acclimatize for one week. Thereafter, they were randomly assigned to the control and treatment groups ( $n = 12$ /control group and 6/treatment group). On the exposure day, the mice were weighed after which they were subjected to a single intratracheal instillation with one of the test substances, each at three dose levels or with a vehicle. Instillation was conducted under isoflurane anesthesia. The mean body weight of mice on the instillation day was  $18.5 \text{ g} \pm 1.4$  (SD). During the post-exposure period, mice were observed twice daily for any abnormalities or for clinical manifestation of adverse reactions.

Post-exposure periods were 1, 3, or 28 d, the animals were anesthetized by subcutaneous injection of the Hypnorm/Dormicum mixture (0.5–0.7 mL/100 g body weight), after which they were killed by collection of heart blood as described previously (Bengtson et al. 2017). The animals were

necropsied: the external surface, all orifices, and thoracic, abdominal, and pelvic cavities including viscera were inspected and any abnormalities if present were noted. The lung and liver samples for comet assay ( $N=6/\text{group}$ ) were collected at necropsy and deep-frozen until analyses.

### **BAL fluid cellularity and genotoxicity**

The BAL procedure, preparation of BAL fluid and examination of BAL fluid cellularity ( $N=6/\text{group}$ ) were performed as previously described (Kyjovska et al. 2015). Tissue preparation and DNA strand break levels quantification using the IMSTAR system were determined as previously described (Jackson et al. 2013).

### **Histological examination of lungs and liver**

Histological examination was done on controls and on the high dose groups ( $2\ \mu\text{g}/\text{mouse}$ ). The lungs were obtained from three randomly selected control mice on termination days 1 and 3, from 4 randomly selected control mice on termination day 28, and from three randomly selected mice from each test material exposed groups on each termination day. The lungs were fixed *in situ* by cannulating the trachea and thereby delivering 4% neutral buffered formaldehyde solution at a constant fluid pressure of 25 cm. Thereafter, the thorax was opened and the lungs were excised and immersed into 4% neutral buffered formaldehyde solution. Livers from four randomly selected controls and three mice from each material high dose group on day 1, 3, and 28 were excised, weighed and specimens were fixed in 4% neutral buffered formaldehyde solution. The lung and liver samples were then processed, embedded in paraffin, sectioned in 4–6  $\mu\text{m}$  thick slices and stained with hematoxylin and eosin (H&E staining) for histological examination by light microscopy in brightfield mode. The examination was performed by two operators, first with knowledge of treatment group identities and thereafter blindly (Haschek, Rousseaux, and Wallig 2010), and following the INHAND proposal for diagnostic nomenclature of microscopic changes in rodents (Renne et al. 2009; Thoolen et al. 2010). Inflammatory cell infiltrates (focal infiltrations of mono- and polynuclear and/or histiocytic cells)

when present in the liver, were divided into two categories: small ( $\leq 10$  inflammatory cells, sporadically accompanied by necrotic hepatocytes with distinct eosinophilic cytoplasm) and big ( $> 10$  inflammatory cells surrounded by necrotic hepatocytes with distinct eosinophilic cytoplasm, with apoptotic bodies/debris often present). The severity scores were given for all changes observed in the lung and for the following changes in the liver: presence of hepatocytes with pyknotic nuclei, cytoplasmic vacuolation of hepatocytes, hyperplasia of connective tissue near bile ductules or venules, hyperplasia of oval cells, apparent increase of Kupffer cells, Kupffer cells with prominent nuclei and apparent increase of binucleate hepatocytes. The severity was evaluated using a 5-grade system: grade 1: minimal/very few/very small; grade 2: mild/few/small; grade 3: moderate/moderate number/moderate size; grade 4: marked/many/large; grade 5: massive/extensive number/extensive size.

### **Total RNA extraction and purification for microarray analysis**

RNA was isolated from random sections of the left lungs ( $n=5$ ) from ZnO-Matrix and Matrix groups using TRIzol reagent (Invitrogen, Carlsbad, CA), and purified with RNeasy Plus Mini kits (Qiagen, Mississauga, Canada) according to the manufacturer's protocol. RNA was quantified using a NanoDrop 2000 spectrophotometer (Thermo Fisher Scientific Inc., Wilmington, DE); RNA quality and integrity were determined with an Agilent 2100 Bioanalyzer (Agilent Technologies, Mississauga, Canada) according to the manufacturer's protocol. All samples had RNA integrity values higher than 7.0.

### **Microarray hybridization**

Double-stranded cDNA was synthesized from 250 ng total RNA of each mouse and from Universal Mouse Reference total RNA (UMRR) (Agilent Technologies, Mississauga, Canada). Cyanine-labeled cRNAs were made from the cDNA with the Quick Amp Labeling Kit (Agilent Technologies, Mississauga, Canada), and then cRNAs from each treatment group were labeled with Cyanine 5-CTP. Reference cRNAs were labeled with Cyanine 3-CTP

in a T7 RNA polymerase *in vitro* transcription kit (Agilent Technologies, Mississauga, Canada). Purification was done with an RNeasy Mini kits (Qiagen, Mississauga, Canada). Each experimental cRNA sample was mixed with an equimolar amount of reference cRNA, and then hybridized to Agilent mouse  $8 \times 60$  k oligonucleotide microarrays (Agilent Technologies Inc., Mississauga, Canada) for 17 h at  $65^\circ\text{C}$  in a hybridization chamber rotating at 10 rpm. Next, the arrays were read in an Agilent G2505B scanner. Gene expression data from the scanned images were processed in the Agilent Feature Extraction software version 9.5.3.1 (Santa Clara, CA, USA).

## Statistics

### *BAL fluid cellularity and DNA strand breaks*

Statistics were calculated in the Graph Pad Prism software package version 7.02 (Graph Pad Software Inc., La Jolla, CA). Data were tested for normality with the Shapiro–Wilk test. The *t*-test and ANOVA are relatively robust against deviations from normality, but somewhat sensitive to differences in standard deviation. We therefore used *t*-test and ANOVA, unless the *p* value of the Shapiro–Wilks test was very low ( $p < 0.001$ ), or standard deviations significantly differed from each other in the *F*-test (for two sample comparisons) or Brown–Forsythe test for three or more treatment groups ( $p < 0.001$ ). The latter tests were conducted because the *t*-test and the ANOVA are somewhat sensitive to differences in standard deviation. In cases with deviations in normality or standard deviations, the non-parametric Mann–Whitney (two groups) or Kruskal–Wallis (more than two groups) tests were used instead. The data were tested so that each material was considered independently against its vehicle control. In order to assess differences in between groups in the one-way ANOVA or Kruskal–Wallis tests, Holm–Sidak’s multiple comparisons test (ANOVA) and Dunn’s multiple comparisons test (Kruskal–Wallis test) were calculated. To test across each material, we calculated the *t*-test or the non-parametric Mann–Whitney test. For this, we tested each dose level of the ZnO-Matrix against the corresponding dose level of ZnO and Matrix. We used a Bonferroni-corrected *p* value adjusted for the six comparisons in the intratracheal instillation study.

The data from microscopic examination of lung and liver were not subjected to statistical analysis due to a low number of the samples.

### *Microarray data*

Microarray data were analyzed as described previously (Husain et al. 2013; Labib et al. 2013; Halappanavar et al. 2015). In brief, a reference randomized block design was employed. Data were normalized using the LOcally WEighted Scatterplot Smoothing (LOWESS) regression modeling method and statistical significance of differentially expressed genes was evaluated using MicroArray ANalysis Of VAriance (MAANOVA) (Rahman et al. 2017) in R statistical software (R Core Team 2012). The *F*<sub>s</sub> statistic (Rahman et al. 2017) was employed to test the treatment effects compared to the control vehicle, and *p* values were estimated by the permutation method using residual shuffling. In order to avoid false positives, false discovery rate (FDR) multiple testing correction (Rahman et al. 2017) was applied. The fold changes of gene expression were determined considering the least-square means. Genes with FDR *p* values of  $\leq 0.05$  were considered significantly differentially expressed, and were included in all downstream analyses. Since the gene list was small, the fold-change-based filtering was not conducted.

## Results

### *Nanoparticle properties*

As agreed with the manufacturer (Nanogate AG, Quierschied, Germany), we do not provide physical-chemical characteristics of the matrix without ZnO. DLS measurements are detailed in Table 1.

### *Pulmonary inflammation determined as the number of BAL fluid neutrophils*

Lung inflammation, in terms of increased neutrophil numbers in BAL fluid, was observed at one and three days post-exposure (Figure 1). At day 1, there was an increase of neutrophils for ZnO at the medium dose level and ZnO-Matrix at both the medium and high dose level, Matrix alone did not increase neutrophil influx at any of the assessed dose levels (Figure 1). At day 3 post-exposure, a clear dose-response relation was seen

**Table 1.** DLS data for the materials.

Material	Z Average size at specific doses (nm)	Polydispersity index (PDI)
ZnO powder Zincor™, also known as NRCWE-031 (here abbreviated ZnO)	2 µg ZnO: 123.9 0.67 µg ZnO: 193.8 0.23 µg ZnO: 652.9	2 µg: 0.27 0.67 µg: 0.48 0.23 µg: 0.67
ZnO in a glass matrix containing approximately 5 wt% ZnO (main solvent ethanol) (Pro.Glass Barrier 401 from Nanogate AG, partner in NanoSustain), also known as NRCWE-029 (here abbreviated ZnO-Matrix)	2 µg ZnO: 189.5 0.67 µg ZnO: 219.4 0.23 µg ZnO: 628.0	2 µg: 0.39 0.67 µg: 0.49 0.23 µg: 0.63
Matrix with no ZnO with the same constituents as Pro.Glass Barrier 401 but without ZnO, also known as NRCWE-039 (here abbreviated Matrix)	Matrix doses had equal amounts of ZnO, while Matrix was adjusted to have an equal volume of matrix as ZnO Matrix. No physico-chemical measurements done	No physico-chemical measurements done
Carbon black Printex 90 (included as a benchmark positive control nanoparticle)	162 µg carbon black: 110.4	0.20

for both ZnO and ZnO-Matrix at medium and high doses (Figure 1). There were differences in the neutrophil levels between ZnO and ZnO-Matrix as well as ZnO-Matrix vs. Matrix when comparing their separate dose levels with *t*-test. At high dose on day 3, ZnO-Matrix had a higher inflammatory response than ZnO, and when comparing several equal dose levels, ZnO-Matrix had a higher inflammatory response than Matrix (Figure 1). No effect was seen for Matrix at any time point, and no effect was seen for any of the ZnO-containing materials at 28 d post-exposure. The benchmark CB Printex-90 induced increased neutrophil influx at all three time-points as previously observed (Figure 1) (Saber et al. 2012a; Poulsen et al. 2016; Bendtsen et al. 2019, 2020; Hadrup et al. 2019, 2020a; Barfod et al. 2020; Danielsen et al. 2020; Hadrup et al. 2021a). Concerning other cell types in the BAL fluid, macrophages and lymphocytes were increased at high doses of ZnO and ZnO-Matrix at day 3, and the latter cell type also at the medium and high dose of ZnO-Matrix at day 1 (Supplemental Materials Figure S1). Total cells had a similar pattern to that of neutrophils (Figure 1).

### **Pulmonary inflammation evaluated by histological examination**

The type, incidence, and severity of histological changes are presented in Supplemental Materials Table S1. Examples of histological changes are presented in Figure 2. Morphological changes indicative of pulmonary inflammation, such as widening of alveolar walls, a local presence of exudate and of leukocytic infiltration in few alveolar lumina were observed both in the control and treatment groups of mice. The severity of these changes was minimal

in the controls while it was slightly increased in single animals from the treatment groups. Furthermore, the onset of these changes was earlier in the treatment groups (day 1 post exposure) than in the controls (day 3 post exposure). These minimal changes in the control mice were considered as a response to the intratracheal instillation with the vehicle. In the mice from the treatment groups, further changes indicative of pulmonary inflammation were seen: leukocytic infiltrations of interstitium, macrophages in alveolar lumina, edema of connective tissue near bronchioles or proliferation of epithelial bronchiolar cells (Supplemental Materials Table S1 and Figure 2). The severity of these changes was similar among the treatment groups being generally minimal although higher severity grades were occasionally assigned to some of these changes. Likewise, incidence of these changes varied to some extent among the mice of the treatment groups at all terminations. E.g. the inflammatory cell infiltrations of the interstitium were observed in all examined mice from the Matrix group on day 1 and from the ZnO group on day 28. Furthermore, extravasation and congestion were observed in the mice from the control and treatment groups. These changes were considered as related to a bleeding of carcasses based on their incidence and severity, although congestion observed post mortem could represent hyperemia that was a part of inflammation.

### **Clinical appearance and liver histology**

No mortality and no difference in the clinical appearance between the control and the exposed mice were seen until the scheduled terminations. Several histological changes were observed in the

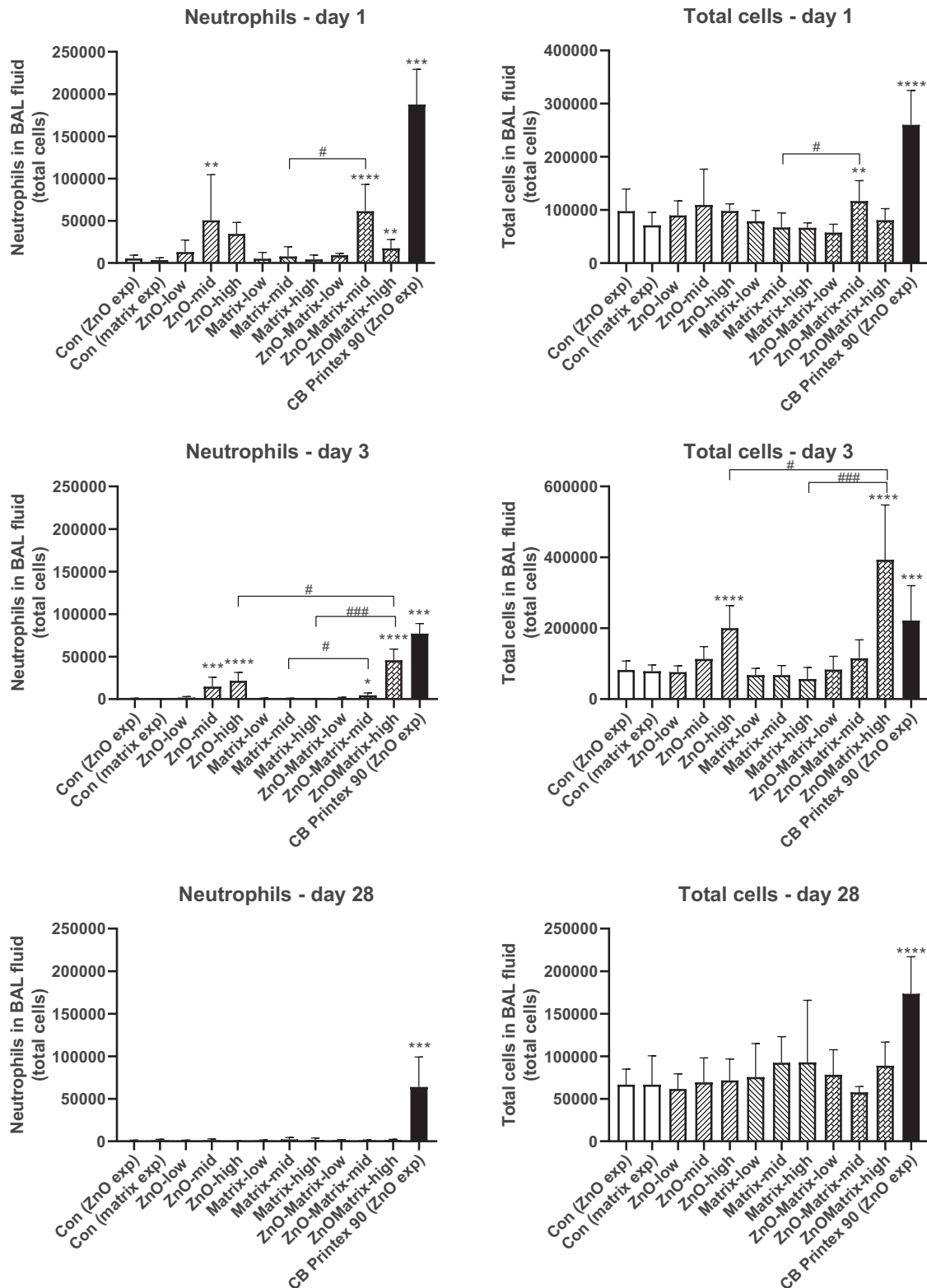


**Figure 1.** Neutrophil and total cell numbers in BAL fluid of mice exposed to the materials. ZnO or ZnO-Matrix were administered by intratracheal instillation at doses providing 0.22, 0.67, or 2  $\mu\text{g}$  ZnO/mouse ( $n = 6/\text{group}$ ). For Matrix, the administered volumes of coating were the same as for the ZnO-matrix. Low, mid, and high designates low dose, mid dose, and high dose, respectively. Carbon black at 162  $\mu\text{g}/\text{mouse}$  ( $n = 6$ ) served as positive control. Data are mean and bars represent SD. \*\*\*, \*\*, and \* designates  $p$  values of  $<0.001$ ,  $<0.01$ , and  $<0.05$ , respectively, of one way ANOVA with Holm-Sidak's multiple comparisons test in case of data approaching normality and not having a highly different variation (details given in the methods section), otherwise by Kruskal-Wallis test with Dunn's multiple comparisons test. In the case of carbon black \*\*\*\*, \*\*\*, \*\*, and \* designates  $p$  values of  $<0.0001$ ,  $<0.001$ ,  $<0.01$ , and  $<0.05$ , respectively, vs. vehicle of the Mann-Whitney test. ### and # designate Bonferroni-corrected (6 comparisons)  $p$  values of  $<0.001$  and  $<0.05$  of unpaired  $t$ -test of ZnO-Matrix vs. ZnO and Matrix.

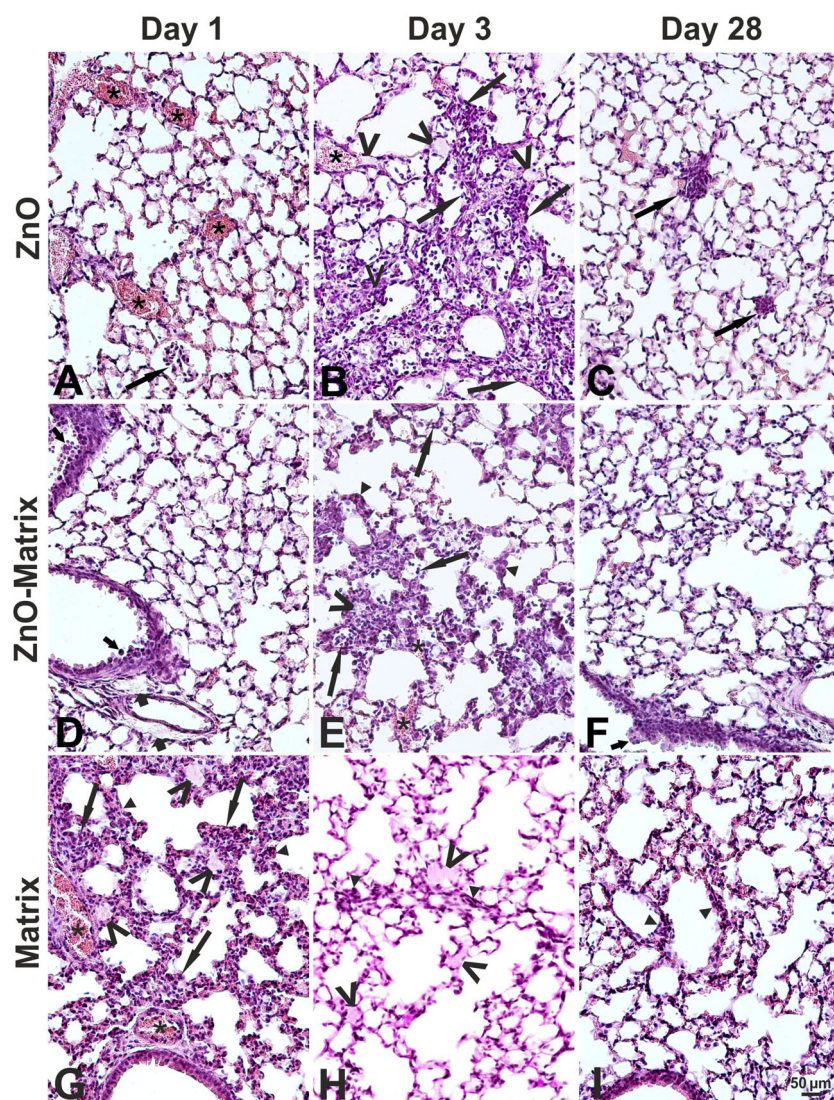


**Figure 2.** Examples of histological changes in the lung of mice on day 1 (A, D, G), 3 (B, E, H), and 28 (C, F, I) after intratracheal instillation with 2  $\mu\text{g}/\text{animal}$  of ZnO (A–C), ZnO-Matrix (D–F), or Matrix (G–I). Asterisks: congestion. Long arrows: leukocytic infiltration in alveolar lumina and walls. Short thin arrows: proliferation of epithelial bronchiolar cells. Short thick arrows: perivascular and peribronchiolar edema. Head arrows: alveolar wall widening. V: exudate in lumen of some alveoli. HE staining, magnification as on the scale in I. An example of a normal structure of the mouse lung is presented in [Supplementary Figure S2\(A\)](#).

examined livers from the control and the treatment groups (Figure 3). The severity of these changes varied from minimal to mild (Table S2). There was no apparent difference in the type of the changes between the control and the treatment groups but the incidence was slightly variable. For example, cytoplasmic vacuolation in hepatocytes (on day 1), hepatocytes with pyknotic nuclei (on day 3), areas of necrosis (on days 1 and 3), and an apparent increase in binucleated hepatocytes (on day 28) were present in all examined livers in ZnO-Matrix group but in fewer or none examined livers from the control or two other treatment groups. In ZnO-

Matrix group, the number of big inflammatory cell infiltrations on days 1 and 3 was elevated as compared to the control and two other treatment groups (Table S3).

### Genotoxicity

We observed only incidental and weak genotoxic effects across doses. In the lung, increased levels of DNA strand breaks expressed as percent of DNA in the comet tail were seen on day 3 post-exposure at low doses of ZnO and ZnO-Matrix, and at the medium dose of Matrix (Figure 4). No effects were

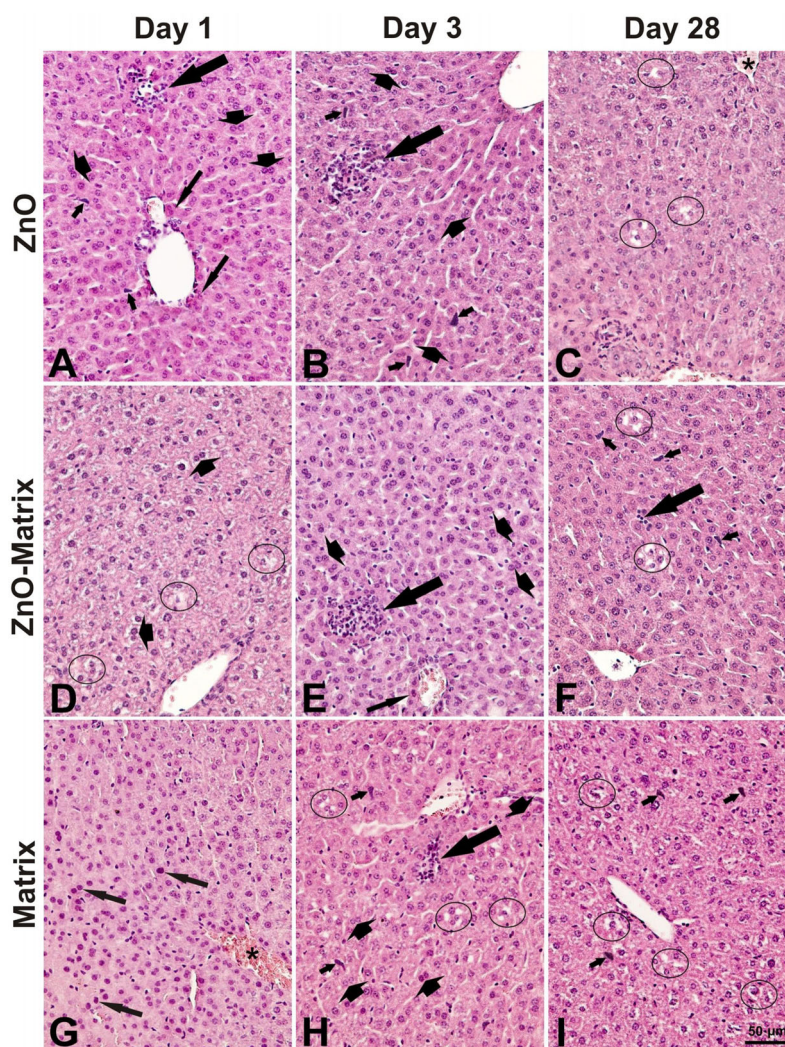


**Figure 3.** Examples of histological changes in the liver day of mice on 1 (A, D, G), 3 (B, E, H), and 28 (C, F, I) after intratracheal instillation of 2 µg/animal of ZnO (A–C), ZnO-Matrix (D–F), or Matrix (G–I). Long thick arrows: focal infiltration of inflammatory cells (note adjacent necrotic hepatocytes with distinct eosinophilic cytoplasm). Long thin arrows: necrotic hepatocytes (in A with eosinophilic cytoplasm, in G with pyknotic nuclei). Short thin arrows: prominent nuclei of Kupffer cells. Short thick arrows: binucleate hepatocytes. Circles: cytoplasmic vacuolation in hepatocytes. Asterisk: congestion. HE staining, magnification as on the scale in I. An example of a normal structure of the mouse liver is presented in [Supplementary Figure S2\(B\)](#).

seen at any other time point in the lung and no effects were seen in the liver ([Supplemental Materials Figure S3](#)).

### Gene expression analysis

Global gene expression profiling was conducted using microarrays to identify the genes and pathways perturbed by ZnO-Matrix exposure as compared to Matrix alone (the bare ZnO was not included in this analysis). In general, the response at the gene expression level was larger in lungs of mice exposed to ZnO-Matrix as compared to the

Matrix alone as seen on day 1 ([Supplemental Materials Figure S4](#)). Effects were virtually absent on day 28 ([Supplemental Materials Figure S4](#)). A further analysis of the differentially expressed genes and the associated canonical pathways revealed that *Circadian Rhythm Signalling*, *Adipogenesis Pathway*, and *Notch Signaling* similarly were activated across doses and treatments ([Figure 5](#)). *Acute Phase Response Signaling* and several other pathways seemed only to be induced by ZnO-Matrix (Low and High dose) and not Matrix alone. ([Figure 5](#)). *Diseases and Functions Affected in Lung Tissue* identified based on the microarray data; as well as

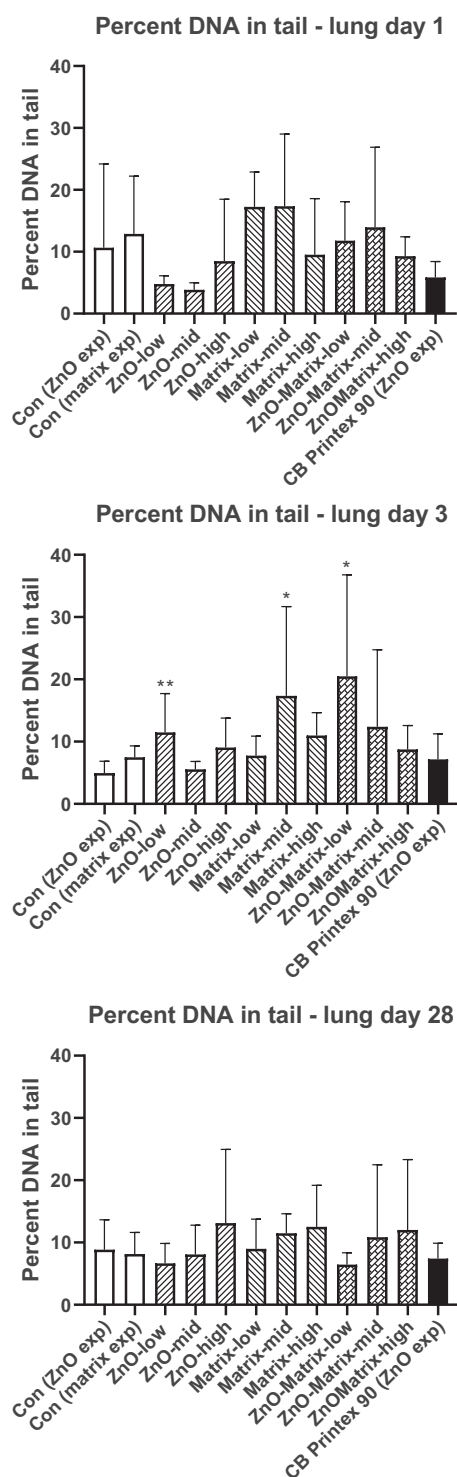


**Figure 4.** Levels of DNA strand breaks in lung tissue at 1, 3, and 28 d of nanoparticle exposure. ZnO or ZnO-Matrix were administered by intratracheal instillation at doses providing 0.22, 0.67, or 2  $\mu\text{g}$  ZnO/mouse ( $n=6$ /group). For Matrix, the same volumes of coating as for the ZnO-matrix were administered. Low, mid, and high designates low dose, mid dose, and high dose, respectively. Carbon black at 162  $\mu\text{g}$ /mouse ( $n=6$ ) served as positive control. Data are mean and bars represent SD. \*\* and \* designates  $p$  values of  $< 0.01$  and  $< 0.05$ , respectively, of one-way ANOVA with Holm-Sidak's multiple comparisons test.

Upstream Regulators Affected in Lung Tissue are found in Supplemental Materials Figures S5 and S6.

## Discussion

In this study, we assessed the toxicity of ZnO nanoparticles in the user-phase, when ZnO was formulated in a liquid matrix for glass coating. This was done by comparing the toxicity of the liquid matrix for glass coating containing ZnO nanoparticle (pro.Glass Barrier 401), with toxicity of the ZnO nanoparticles alone and the liquid matrix with no ZnO, following pulmonary exposure in mice, using a previously published experimental set-up (Saber et al. 2012a, 2016, 2019). We assessed the dose-response relations of inflammation and DNA damage 1, 3, and 28 d after a single intratracheal instillation in mice, performed gene expression analysis on the lung tissue and evaluated effect by microscopy effect of exposure to the test materials in the lung and in the liver.

## Tested material, study design, and dose considerations

We chose to study a surface coating containing approximately 5% ZnO nanoparticle (pro.Glass Barrier 401). This is a solvent-borne one-component lacquer system, which is applied by dip, flow or knife coating. When cured it blocks a substantial part of the UV radiation (Luther and Zweck 2013).

Mice were exposed by intratracheal instillation. The gold standard for risk assessment of pulmonary exposure is inhalation. However, intratracheal instillation has the advantage that it allows control of the biological dose, and it is therefore useful for comparison of hazard potential (Bendtsen et al. 2020). Furthermore, we have previously demonstrated that nanoparticles dosed by intratracheal instillation reach all lung lobes in mice (Mikkelsen et al. 2011; Poulsen et al. 2016).

The dose levels of the pristine ZnO nanoparticle, 0.22, 0.67, and 2  $\mu\text{g}$ , were chosen based on a previous study of the same ZnO nanoparticle where it was found that 2  $\mu\text{g}$  ZnO was the highest dose with no overt toxicity (no decrease in body weight was observed for 2  $\mu\text{g}$  ZnO NP) (Jacobsen et al. 2015). To be able to compare the toxicity of the ZnO-containing glass matrix coating with the toxicity of the

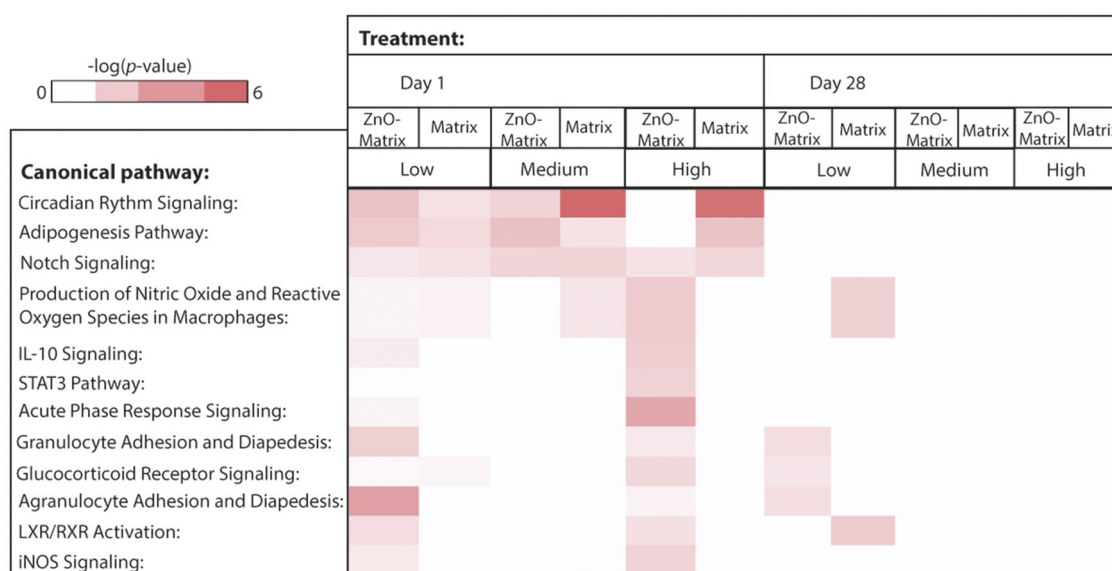


**Figure 5.** Canonical pathways affected in lung tissue by 1 or 28 d of ZnO-Matrix or Matrix exposure. ZnO-Matrix or Matrix was administered by intratracheal instillation at 0.22, 0.67, or 2  $\mu\text{g}/\text{mouse}$  (designated: low, medium, and high). The deeper the red coloring is, the higher the effect is on the specific canonical pathway. The bare ZnO nanoparticle was not tested in this assay.

ZnO nanoparticles, we exposed the mice to the glass matrix coating containing the similar amounts of ZnO as the doses of the pristine ZnO nanoparticles. For the evaluation of the toxicity of the glass matrix alone, we included the glass matrix coating without ZnO and used the same doses (volumes) as for the ZnO-containing glass matrix product. We tested the matrix coatings in their liquid form before application and curing (the true user-phase). In that way, we tested a model of the scenario of occupational exposure during the coating process. Another relevant scenario could have been to test sanding dusts obtained during sanding of the cured glass matrices as we have done in previous assessments of paints and epoxy-composites containing nanoparticles (Saber et al. 2012a, 2012c, 2016, 2019). However, in this case, it was not possible to generate and collect enough dust for the toxicological tests when sanding the cured coating (results not shown).

The tested time points (1, 3, and 28 d) were similar to those in our previous studies on sanding dusts from paints with and without nano titanium dioxide ( $\text{NanoTiO}_2$ ) (Saber et al. 2012a, 2019) and epoxy with and without carbon nanotubes (Saber et al. 2016). In these studies, the toxicity of  $\text{NanoTiO}_2$  was markedly reduced when embedded in a paint matrix (Saber et al. 2012a, 2019). Similarly, the pulmonary toxicity of MWCNT was

reduced when embedded in an epoxy matrix (Saber et al. 2016).

### **ZnO and ZnO-Matrix exhibit similar toxicity**

The similar dose levels of nanoparticles in the ZnO and ZnO-Matrix groups (and the similar volume of matrix in the Matrix group) enabled assessment of whether inclusion of ZnO nanoparticles in a glass matrix coating modifies ZnO toxicity. Both ZnO and ZnO-Matrix induced lung inflammation in terms of neutrophil influx, while Matrix (at the same matrix volume as ZnO-Matrix) had no effect. On day 3 post-exposure, there was a dose-response relationship in the neutrophil influx for ZnO and ZnO-Matrix and the influx induced by ZnO-Matrix was larger (for the highest dose level) or similar (for the middle dose level) to the influx induced by ZnO nanoparticles. Also, the histological examination, revealed a similar pulmonary inflammation in ZnO and ZnO-Matrix groups on day 3 (Figure 2(B,E)). Thus, overall, we found that ZnO and ZnO Matrix had comparable toxicity, demonstrating that ZnO toxicity was unaffected by the suspension of ZnO particles in a glass surface coating product. This is in contrast to what has been reported for other nanocomposites, for example in the study by Wohlleben et al. (2011) and previous studies by our group. In these studies, addition of nanoparticles to paints/

lacquer (Saber et al. 2012a, 2016) and epoxy matrices (Wohlleben et al. 2011; Saber et al. 2016) did not affect the toxicity of sanding dust of the materials. Thus, the toxicity of the nanoparticles was reduced after being incorporated into a matrix. In the previously mentioned studies, the nanoparticles were assessed as sanding dust of a matrix containing encapsulated nanoparticles. In this study, we tested the toxicity of the uncured material in liquid form before application. One could anticipate that ZnO would be more accessible in the liquid matrix following instillation as compared to nanoparticle accessibility in sanding dust. This may explain the similar toxicity of ZnO alone and in the liquid matrix.

Overall, there was no increased toxicity of embedding ZnO in the glass matrix. Our other concern was a possibility of enhanced toxic potential in the form of synergy when combining materials. Yet, the inflammatory response in terms of BAL cell composition and as evaluated by histological examination was consistent with additive effects of ZnO and Matrix. Thus, potential for a synergistic effect that could enhance toxicity when combining ZnO and Matrix into one product was ruled out.

#### ***Microarray data and their contribution to the understanding of toxicity endpoints activated by ZnO and the underlying mechanisms***

Assessment of the global pulmonary gene expression can contribute to the understanding of the mechanism of toxicity of ZnO. A gene-array study on lung tissue from the mice instilled with ZnO-Matrix and Matrix demonstrated that ZnO-Matrix induced substantially more differential gene expression than Matrix. This corroborated that the ZnO had a stronger impact on the mouse lung than its accompanying material. The response at the gene expression level suggested possibility of inflammation, disturbance in lipid metabolism, cardiovascular diseases, cancer, and circadian rhythm perturbation. This is in line with the inflammation observed in this study as well as inflammation observed in several previous studies (Ho et al. 2011; Adamcakova-Dodd et al. 2014; Chuang et al. 2014; Chen et al. 2015; Larsen et al. 2016) and with the activation of the acute phase response marker SAA (Monsé et al. 2018; Hadrup et al. 2019). This marker has by

persistent or recurring activation been linked to increased risk of cardiovascular disease (Ridker et al. 2000; Saber et al. 2013, 2014; Hadrup et al. 2020b).

#### ***Contribution to the understanding of the general toxicity of ZnO***

The toxicity seen at 0.67 and 2 µg ZnO/mouse in terms of increased BAL fluid neutrophil numbers on day 3 suggests a NOAEL of 0.22 µg/mouse equivalent to ~0.01 mg/kg bw. In a previous study of two different ZnO particles, 0.7 µg/mouse (~0.03 mg/kg bw) was identified as the NOAEL for an uncoated ZnO nanoparticle and 0.2 µg/mouse (~0.01 mg/kg bw) for a triethoxycaprylylsilane-coated ZnO nanoparticle (Hadrup et al. 2019). Other intratracheal studies have been done with doses higher than the above-described ones, as well as higher than the ones used in this study. These NOAELs were 0.17 mg/kg bw in mice (Jacobsen et al. 2015), and 0.1 mg/kg bw in rats (Rice et al. 2001). Likewise, LOAELs were in the range of 0.3–1 mg/kg bw in rat and mouse (Warheit, Sayes, and Reed 2009; Cho et al. 2010, 2011, 2012; Jacobsen et al. 2015). Concerning inhalation studies with ZnO nanoparticles in rodents, increased pulmonary inflammation in the form of increased neutrophil numbers in BAL fluid gave NOAECs in the range of 0.4–7 mg/m<sup>3</sup> (Ho et al. 2011; Adamcakova-Dodd et al. 2014; Chuang et al. 2014; Chen et al. 2015; Larsen et al. 2016).

Concerning histological examination of the liver, we found no apparent differences in the type of changes between the control and the test materials groups (Table S2); although some of the changes in the exposed groups were previously reported after intratracheal exposure of mice to 2 µg ZnO (Jacobsen et al. 2015). Most of the observed changes belong either to a background pathology of the mouse (i.e. that may occur spontaneously), or as a result of toxicant insult (Harada et al. 1999). This also relates to the inflammatory cell infiltrations which were present in the controls and the test material exposed groups. However, the noteworthy finding was a transient increase in the number of big inflammatory cell infiltrations in ZnO-Matrix group on day 1 (when the pulmonary acute phase response is expected to be present) and on day 3 post-exposure (when the pulmonary inflammation was the strongest based on the neutrophil influx

and histology) (Table S3). This suggests an exacerbation of spontaneous inflammatory processes in the liver possibly related to an acute phase response/a systemic inflammatory response that accompany pulmonary inflammation after intratracheal instillation. Indeed, biomarkers of the acute phase response/inflammation were significantly elevated already day 1 after intratracheal exposure to different nanomaterials. This was also the case for plasma levels of serum amyloid A3 (SAA3) in mice exposed to multiwall carbon nanotubes (Poulsen et al. 2015), pulmonary expression of *Saa3* mRNA in mice exposed to certain nanoclays (Di Ianni et al. 2020) or pulmonary and hepatic expression of *Saa3* mRNA in mice exposed to TiO<sub>2</sub> and CeO<sub>2</sub> nanoparticles (Modrzynska et al. 2018). The latter deserves further investigations as the inflammatory liver changes have been reported after pulmonary exposure to different nanomaterials, e.g. (Cui et al. 2010; Nalabotu et al. 2011; Saber et al. 2012b; Hougaard et al. 2013; Xu et al. 2013; Jacobsen et al. 2015; Saber et al. 2016, 2019).

The limited genotoxic potential demonstrated in the comet assay in this study, is in line with our previous findings on uncoated and coated ZnO nanoparticles (Hadrup et al. 2019), and as outlined in the introduction the data on a genotoxic potential of ZnO are inconsistent (Ho et al. 2011; Chuang et al. 2014; Larsen et al. 2016).

## Conclusion

Under conditions of this study and based on endpoints evaluated, we conclude that the toxicity of ZnO persisted when included in a liquid matrix for glass coating as a similar pattern of toxicity was seen for ZnO and ZnO-Matrix.

## Acknowledgments

The authors greatly acknowledge the excellent technical assistance of Lourdes Pedersen, Elzbieta Christiansen, Michael Guldbrandsen, Eva Terrida, Lisbeth Pedersen, Yahia Kembouche, and Anne-Karin Asp; and we thank Aleksander Penkowski for preparing the histology figures. Authors acknowledge funding received from Health Canada's Genomics Research and Development Initiative.

## Disclosure statement

Alexander Kurz is an employee of Techniplas NAG GmbH, which developed the studied ZnO Matrix and Matrix. The other authors report no competing interest.

## Funding

This article is part of the NanoSustain project funded by the European Community's Seventh Framework Programme (FP7/2007-2013) under grant agreement n° 247989 (Nanosustain). Furthermore, the work is supported by the PaTROLSproject funded by the European Union's Horizon 2020 research and innovation programme under grant agreement No 760813 and the FFIKA, Focused Research Effort on Chemicals in the Working Environment, from the Danish Government. Authors acknowledge funding received from Health Canada's Genomics Research and Development Initiative.

## ORCID

Niels Hadrup  <http://orcid.org/0000-0002-1188-445X>

Nicklas Raun Jacobsen  <http://orcid.org/0000-0002-2504-2229>

Håkan Wallin  <http://orcid.org/0000-0001-7716-0166>

Ulla Vogel  <http://orcid.org/0000-0001-6807-1524>

## References

- Adamcakova-Dodd, A., L. V. Stebounova, J. S. Kim, S. U. Vorrink, A. P. Ault, P. T. O'Shaughnessy, V. H. Grassian, and P. S. Thorne. 2014. "Toxicity Assessment of Zinc Oxide Nanoparticles Using Sub-Acute and Sub-Chronic Murine Inhalation Models." *Part Fibre.Toxicol* 11 (1743-8977): 15. doi:10.1186/1743-8977-11-15
- Barfod, K. K., K. M. Bendtsen, T. Berthing, A. J. Koivisto, S. S. Poulsen, E. Segal, E. Verleysen, et al. 2020. "Increased Surface Area of Halloysite Nanotubes Due to Surface Modification Predicts Lung Inflammation and Acute Phase Response after Pulmonary Exposure in Mice." *Environmental Toxicology and Pharmacology* 73: 103266. doi:10.1016/j.etap.2019.103266.
- Beckett, W. S., D. F. Chalupa, A. Pauly-Brown, D. M. Speers, J. C. Stewart, M. W. Frampton, M. J. Utell, et al. 2005. "Comparing Inhaled Ultrafine versus Fine Zinc Oxide Particles in Healthy Adults: A Human Inhalation Study." *American Journal of Respiratory and Critical Care Medicine* 171 (10): 1129-1135. doi:10.1164/rccm.200406-837OC.
- Bendtsen, K. M., A. Brostrøm, A. J. Koivisto, I. Koponen, T. Berthing, N. Bertram, K. I. Kling, et al. 2019. "Airport Emission Particles: Exposure Characterization and Toxicity following Intratracheal Instillation in Mice." *Particle and Fibre Toxicology* 16 (1): 23. doi:10.1186/s12989-019-0305-5.
- Bendtsen, K. M., L. Gren, V. B. Malmborg, P. C. Shukla, M. Tunér, Y. J. Essig, A. M. Kraus, et al. 2020. "Particle

- Characterization and Toxicity in C57BL/6 Mice following Instillation of Five Different Diesel Exhaust Particles Designed to Differ in Physicochemical Properties." *Particle and Fibre Toxicology* 17 (1): 38. doi:10.1186/s12989-020-00369-9
- Bengtson, S., K. B. Knudsen, Z. O. Kyjovska, T. Berthing, V. Skaug, M. Levin, I. K. Koponen, et al. 2017. "Differences in Inflammation and Acute Phase Response but Similar Genotoxicity in Mice following Pulmonary Exposure to Graphene Oxide and Reduced Graphene Oxide." *PLoS One* 12 (6): e0178355. doi:10.1371/journal.pone.0178355.
- Chen, J. K., C. C. Ho, H. Chang, J. F. Lin, C. S. Yang, M. H. Tsai, H. T. Tsai, and P. Lin. 2015. "Particulate Nature of Inhaled Zinc Oxide Nanoparticles Determines Systemic Effects and Mechanisms of Pulmonary Inflammation in Mice." *Nanotoxicology* 9 (1): 43–53. doi:10.3109/17435390.2014.886740.
- Cho, W. S., R. Duffin, S. E. Howie, C. J. Scotton, W. A. Wallace, W. MacNee, M. Bradley, I. L. Megson, and K. Donaldson. 2011. "Progressive Severe Lung Injury by Zinc Oxide Nanoparticles; the Role of Zn<sup>2+</sup> Dissolution inside Lysosomes." *Particle and Fibre Toxicology* 8 (1743–8977): 27.
- Cho, W. S., R. Duffin, C. A. Poland, A. Duschl, G. J. Oostingh, W. MacNee, M. Bradley, I. L. Megson, and K. Donaldson. 2012. "Differential Pro-Inflammatory Effects of Metal Oxide Nanoparticles and Their Soluble Ions in Vitro and in Vivo; Zinc and Copper Nanoparticles, but Not Their Ions, Recruit Eosinophils to the Lungs." *Nanotoxicology* 6 (1): 22–35. doi:10.3109/17435390.2011.552810.
- Cho, W. S., R. Duffin, C. A. Poland, S. E. Howie, W. MacNee, M. Bradley, I. L. Megson, and K. Donaldson. 2010. "Metal Oxide Nanoparticles Induce Unique Inflammatory Footprints in the Lung: Important Implications for Nanoparticle Testing." *Environmental Health Perspectives* 118 (12): 1699–1706. doi:10.1289/ehp.1002201.
- Chuang, H. C., H. T. Juan, C. N. Chang, Y. H. Yan, T. H. Yuan, J. S. Wang, H. C. Chen, Y. H. Hwang, C. H. Lee, and T. J. Cheng. 2014. "Cardiopulmonary Toxicity of Pulmonary Exposure to Occupationally Relevant Zinc Oxide Nanoparticles." *Nanotoxicology* 8 (6): 593–604. doi:10.3109/17435390.2013.809809.
- Cooper, M. R., G. H. West, L. G. Burrelli, D. Dresser, K. N. Griffin, A. M. Segrave, J. Perrenoud, and B. E. Lippy. 2017. "Inhalation Exposure during Spray Application and Subsequent Sanding of a Wood Sealant Containing Zinc Oxide Nanoparticles." *Journal of Occupational and Environmental Hygiene* 14 (7): 510–522. doi:10.1080/15459624.2017.1296237.
- Cui, Y., X. Gong, Y. Duan, N. Li, R. Hu, H. Liu, M. Hong, et al. 2010. "Hepatocyte Apoptosis and Its Molecular Mechanisms in Mice Caused by Titanium Dioxide Nanoparticles." *Journal of Hazardous Materials* 183 (1–3): 874–880. doi:10.1016/j.jhazmat.2010.07.109.
- Danielsen, P. H., K. B. Knudsen, J. Štrancar, P. Umek, T. Koklič, M. Garvas, E. Vanhala, et al. 2020. "Effects of Physicochemical Properties of TiO<sub>2</sub> Nanomaterials for Pulmonary Inflammation, Acute Phase Response and Alveolar Proteinosis in Intratracheally Exposed Mice." *Toxicology and Applied Pharmacology* 386: 114830. doi:10.1016/j.taap.2019.114830.
- Di Ianni, E., P. Møller, A. Mortensen, J. Szarek, P. A. Clausen, A. T. Saber, U. Vogel, and N. R. Jacobsen. 2020. "Organomodified Nanoclays Induce Less Inflammation, Acute Phase Response, and Genotoxicity than Pristine Nanoclays in Mice Lungs." *Nanotoxicology* 14 (7): 869–892. doi:10.1080/17435390.2020.1771786.
- Greenberg, M. I., and D. Vearrier. 2015. "Metal Fume Fever and Polymer Fume Fever." *Clinical Toxicology (Philadelphia, PA)* 53 (4): 195–203. doi:10.3109/15563650.2015.1013548.
- Hadrup, N., K. Aimonen, M. Ilves, H. Lindberg, R. Atluri, N. M. Sahlgren, N. R. Jacobsen, et al. 2021a. "Pulmonary Toxicity of Synthetic Amorphous Silica - Effects of Porosity and Copper Oxide Doping." *Nanotoxicology* 15 (1): 96–113. doi:10.1080/17435390.2020.1842932.
- Hadrup, N., S. Bengtson, N. R. Jacobsen, P. Jackson, M. Nocun, A. T. Saber, K. A. Jensen, H. Wallin, and U. Vogel. 2017. "Influence of Dispersion Medium on Nanomaterial-Induced Pulmonary Inflammation and DNA Strand Breaks: Investigation of Carbon Black, Carbon Nanotubes and Three Titanium Dioxide Nanoparticles." *Mutagenesis* 32 (6): 581–597. doi:10.1093/mutage/gex042
- Hadrup, N., F. Rahmani, N. R. Jacobsen, A. T. Saber, P. Jackson, S. Bengtson, A. Williams, H. Wallin, S. Halappanavar, and U. Vogel. 2019. "Acute Phase Response and Inflammation following Pulmonary Exposure to Low Doses of Zinc Oxide Nanoparticles in Mice." *Nanotoxicology* 13 (9): 1275–1292. doi:10.1080/17435390.2019.1654004
- Hadrup, N., A. Saber, N. Jacobsen, P. Danielsen, S. Poulsen, K. Hougaard, and U. Vogel. 2021b. *Zinc Oxide: Scientific Basis for Setting a Health-based Occupational Exposure Limit*. Copenhagen, Denmark: The National Research Centre for the Working Environment (NFA).
- Hadrup, N., A. T. Saber, Z. O. Kyjovska, N. R. Jacobsen, M. Vippola, E. Sarlin, Y. Ding, et al. 2020a. "Pulmonary Toxicity of Fe<sub>2</sub>O<sub>3</sub>, ZnFe<sub>2</sub>O<sub>4</sub>, NiFe<sub>2</sub>O<sub>4</sub> and NiZnFe<sub>4</sub>O<sub>8</sub> Nanomaterials: Inflammation and DNA Strand Breaks." *Environmental Toxicology and Pharmacology* 74: 103303. doi:10.1016/j.etap.2019.103303.
- Hadrup, N., V. Zhernovkov, N. R. Jacobsen, C. Voss, M. Strunz, M. Ansari, H. B. Schiller, et al. 2020b. "Acute Phase Response as a Biological Mechanism-of-Action of (Nano)Particle-Induced Cardiovascular Disease." *Small* 16 (21): 1907476. doi:10.1002/smll.201907476
- Halappanavar, S., A. T. Saber, N. Decan, K. A. Jensen, D. Wu, N. R. Jacobsen, C. Guo, et al. 2015. "Transcriptional Profiling Identifies Physicochemical Properties of Nanomaterials That Are Determinants of the in Vivo Pulmonary Response." *Environmental and Molecular Mutagenesis* 56 (2): 245–264. doi:10.1002/em.21936.
- Harada, T., A. Enomoto, G. A. Boorman, and R. Maronpot. 1999. "Liver and Gallbladder." In *Pathology of the Mouse*,

- edited by R. Maronpot, G.A. Boorman, and B.W. Gaul, 119–183. Saint Louis, MO: Cache River Press.
- Haschek, W., C. Rousseaux, and M. Wallig. 2010. *Fundamentals of Toxicologic Pathology*. 2nd ed. Amsterdam, Netherlands: Elsevier Academic Press.
- Ho, M., K. Y. Wu, H. M. Chein, L. C. Chen, and T. J. Cheng. 2011. "Pulmonary Toxicity of Inhaled Nanoscale and Fine Zinc Oxide Particles: Mass and Surface Area as an Exposure Metric." *Inhalation Toxicology* 23 (14): 947–956. doi:10.3109/08958378.2011.629235.
- Hougaard, K. S., P. Jackson, Z. O. Kyjovska, R. K. Birkedal, P. J. De Temmerman, A. Brunelli, E. Verleysen, et al. 2013. "Effects of Lung Exposure to Carbon Nanotubes on Female Fertility and Pregnancy. A Study in Mice." *Reproductive Toxicology (Elmsford, NY)* 41 (1873–1708): 86–97. doi:10.1016/j.reprotox.2013.05.006.
- Husain, M., A. T. Saber, C. Guo, N. R. Jacobsen, K. A. Jensen, C. L. Yauk, A. Williams, U. Vogel, H. Wallin, and S. Halappanavar. 2013. "Pulmonary Instillation of Low Doses of Titanium Dioxide Nanoparticles in Mice Leads to Particle Retention and Gene Expression Changes in the Absence of Inflammation." *Toxicology and Applied Pharmacology* 269 (3): 250–262. doi:10.1016/j.taap.2013.03.018.
- Jackson, P., L. M. Pedersen, Z. O. Kyjovska, N. R. Jacobsen, A. T. Saber, K. S. Hougaard, U. Vogel, and H. Wallin. 2013. "Validation of freezing tissues and cells for analysis of DNA strand break levels by comet assay." *Mutagenesis* 28 (6): 699–707.
- Jackson, P., S. P. Lund, G. Kristiansen, O. Andersen, U. Vogel, H. Wallin, and K. S. Hougaard. 2011. "An Experimental Protocol for Maternal Pulmonary Exposure in Developmental Toxicology." *Basic & Clinical Pharmacology & Toxicology* 108 (3): 202–207. doi:10.1111/j.1742-7843.2010.00644.x.
- Jacobsen, N. R., T. Stoeger, B. S. van den, A. T. Saber, A. Beyerle, G. Vietti, A. Mortensen, et al. 2015. "Acute and Subacute Pulmonary Toxicity and Mortality in Mice after Intratracheal Instillation of ZnO Nanoparticles in Three Laboratories." *Food and Chemical Toxicology: An International Journal Published for the British Industrial Biological Research Association* 85 (1873–6351): 84–95. doi:10.1016/j.fct.2015.08.008.
- Jensen, K. A., and Y. Kembouche. 2014. *The ENPRA Dispersion Protocol for NANoREG*.
- Kyjovska, Z. O., N. R. Jacobsen, A. T. Saber, S. Bengtson, P. Jackson, H. Wallin, and U. Vogel. 2015. "DNA Damage following Pulmonary Exposure by Instillation to Low Doses of Carbon Black (Printex 90) Nanoparticles in Mice." *Environmental and Molecular Mutagenesis* 56 (1): 41–49. doi:10.1002/em.21888.
- Labib, S., C. H. Guo, A. Williams, C. L. Yauk, P. A. White, and S. Halappanavar. 2013. "Toxicogenomic Outcomes Predictive of Forestomach Carcinogenesis following Exposure to Benzo(a)Pyrene: Relevance to Human Cancer Risk." *Toxicology and Applied Pharmacology* 273 (2): 269–280. doi:10.1016/j.taap.2013.05.027.
- Larsen, S. T., P. Jackson, S. S. Poulsen, M. Levin, K. A. Jensen, H. Wallin, G. D. Nielsen, and I. K. Koponen. 2016. "Airway Irritation, Inflammation, and Toxicity in Mice following Inhalation of Metal Oxide Nanoparticles." *Nanotoxicology* 10 (9): 1254–1262. doi:10.1080/17435390.2016.1202350.
- Luther, W., and A. Zweck. 2013. *Safety Aspects of Engineered Nanomaterials*. Boca Raton, FL: CRC Press.
- Mikkelsen, L., M. Sheykhzade, K. A. Jensen, A. T. Saber, N. R. Jacobsen, U. Vogel, H. Wallin, S. Loft, and P. Moller. 2011. "Modest Effect on Plaque Progression and Vasodilatory Function in Atherosclerosis-Prone Mice Exposed to Nanosized TiO<sub>2</sub>." *Particle and Fibre Toxicology* 8 (1743–8977): 32.
- Modrzynska, J., T. Berthing, G. Ravn-Haren, N. R. Jacobsen, I. K. Weydahl, K. Loeschner, A. Mortensen, A. T. Saber, and U. Vogel. 2018. "Primary Genotoxicity in the Liver following Pulmonary Exposure to Carbon Black Nanoparticles in Mice." *Particle and Fibre Toxicology* 15 (1): 2. doi:10.1186/s12989-017-0238-9.
- Monsé, C., O. Hagemeyer, M. Raulf, B. Jettkant, V. van Kampen, B. Kendzia, V. Gering, et al. 2018. "Concentration-Dependent Systemic Response after Inhalation of Nano-Sized Zinc Oxide Particles in Human Volunteers." *Particle and Fibre Toxicology* 15 (1): 8. doi:10.1186/s12989-018-0246-4.
- Monsé, C., M. Raulf, B. Jettkant, V. van Kampen, B. Kendzia, L. Schürmeyer, C. E. Seifert, et al. 2021. "Health Effects after Inhalation of Micro- and Nano-Sized Zinc Oxide Particles in Human Volunteers." *Archives of Toxicology* 95 (1): 53–65. doi:10.1007/s00204-020-02923-y.
- Nalabotu, S. K., H. Addagarla, K. Triest, M. M. Katta, and R. Blough. 2011. "Intratracheal Instillation of Cerium Oxide Nanoparticles Induces Hepatic Toxicity in Male Sprague-Dawley Rats." *International Journal of Nanomedicine* 6: 2327. doi:10.2147/IJN.S25119
- Ogura, I., H. Sakurai, and M. Gamo. 2011. "Onsite Aerosol Measurements for Various Engineered Nanomaterials at Industrial Manufacturing Plants." *Journal of Physics: Conference Series* 304: 012004. doi:10.1088/1742-6596/304/1/012004
- Poulsen, S. S., P. Jackson, K. Kling, K. B. Knudsen, V. Skaug, Z. O. Kyjovska, B. L. Thomsen, et al. 2016. "Multi-Walled Carbon Nanotube Physicochemical Properties Predict Pulmonary Inflammation and Genotoxicity." *Nanotoxicology* 10 (9): 1263–1275. doi:10.1080/17435390.2016.1202351.
- Poulsen, S. S., A. T. Saber, A. Mortensen, J. Szarek, D. Wu, A. Williams, O. Andersen, et al. 2015. "Changes in Cholesterol Homeostasis and Acute Phase Response Link Pulmonary Exposure to Multi-Walled Carbon Nanotubes to Risk of Cardiovascular Disease." *Toxicology and Applied Pharmacology* 283 (3): 210–222. doi:10.1016/j.taap.2015.01.011.
- R Core Team. 2012. *R: A Language and Environment for Statistical Computing*. Vienna, Austria: R Foundation for Statistical Computing.
- Rahman, L., N. R. Jacobsen, S. A. Aziz, D. Wu, A. Williams, C. L. Yauk, P. White, H. Wallin, U. Vogel, and S.

- Halappanavar. 2017. "Multi-Walled Carbon Nanotube-Induced Genotoxic, Inflammatory and Pro-Fibrotic Responses in Mice: Investigating the Mechanisms of Pulmonary Carcinogenesis." *Mutation Research Genetic Toxicology and Environmental Mutagenesis* 823: 28–44. doi:10.1016/j.mrgentox.2017.08.005.
- Renne, R., A. Brix, J. Harkema, R. Herbert, B. Kittel, D. Lewis, T. March, et al. 2009. "Proliferative and Nonproliferative Lesions of the Rat and Mouse Respiratory Tract." *Toxicologic Pathology* 37 (7): 55–73S. doi:10.1177/0192623309353423.
- Rice, T. M., R. W. Clarke, J. J. Godleski, E. Al-Mutairi, N. F. Jiang, R. Hauser, and J. D. Paulauskis. 2001. "Differential Ability of Transition Metals to Induce Pulmonary Inflammation." *Toxicology and Applied Pharmacology* 177 (1): 46–53. doi:10.1006/taap.2001.9287.
- Ridker, P. M., C. H. Hennekens, J. E. Buring, and N. Rifai. 2000. "C-Reactive Protein and Other Markers of Inflammation in the Prediction of Cardiovascular Disease in Women." *The New England Journal of Medicine* 342 (12): 836–843. doi:10.1056/NEJM200003233421202.
- Saber, A. T., N. R. Jacobsen, P. Jackson, S. S. Poulsen, Z. O. Kyjovska, S. Halappanavar, C. L. Yauk, H. Wallin, and U. Vogel. 2014. "Particle-Induced Pulmonary Acute Phase Response May Be the Causal Link between Particle Inhalation and Cardiovascular Disease." *Wiley Interdisciplinary Reviews Nanomedicine and Nanobiotechnology* 6 (6): 517–531. doi:10.1002/wnan.1279.
- Saber, A. T., N. R. Jacobsen, A. Mortensen, J. Szarek, P. Jackson, A. M. Madsen, K. A. Jensen, et al. 2012a. "Nanotitanium Dioxide Toxicity in Mouse Lung is Reduced in Sanding Dust from Paint." *Particle and Fibre Toxicology* 9 (1743–8977): 4. doi:10.1186/1743-8977-9-4.
- Saber, A. T., K. A. Jensen, N. R. Jacobsen, R. Birkedal, L. Mikkelsen, P. Moller, S. Loft, H. Wallin, and U. Vogel. 2012b. "Inflammatory and Genotoxic Effects of Nanoparticles Designed for Inclusion in Paints and Lacquers." *Nanotoxicology* 6 (5): 453–471. doi:10.3109/17435390.2011.587900.
- Saber, A. T., I. K. Koponen, K. A. Jensen, N. R. Jacobsen, L. Mikkelsen, P. Moller, S. Loft, U. Vogel, and H. Wallin. 2012c. "Inflammatory and Genotoxic Effects of Sanding Dust Generated from Nanoparticle-Containing Paints and Lacquers." *Nanotoxicology* 6 (7): 776–788. doi:10.3109/17435390.2011.620745.
- Saber, A. T., J. S. Lamson, N. R. Jacobsen, G. Ravn-Haren, K. S. Hougaard, A. N. Nyendi, P. Wahlberg, et al. 2013. "Particle-Induced Pulmonary Acute Phase Response Correlates with Neutrophil Influx Linking Inhaled Particles and Cardiovascular Risk." *PLoS One* 8 (7): e69020. doi:10.1371/journal.pone.0069020.
- Saber, A. T., A. Mortensen, J. Szarek, N. R. Jacobsen, M. Levin, I. K. Koponen, K. A. Jensen, U. Vogel, and H. Wallin. 2019. "Toxicity of Pristine and Paint-Embedded TiO<sub>2</sub> Nanomaterials." *Human & Experimental Toxicology* 38 (1): 11–24. doi:10.1177/0960327118774910.
- Saber, A. T., A. Mortensen, J. Szarek, I. K. Koponen, M. Levin, N. R. Jacobsen, M. E. Pozzebbon, et al. 2016. "Epoxy Composite Dusts with and without Carbon Nanotubes Cause Similar Pulmonary Responses, but Differences in Liver Histology in Mice following Pulmonary Deposition." *Particle and Fibre Toxicology* 13 (1): 37. doi:10.1186/s12989-016-0148-2.
- Shi, J., Karlsson, H. L., K. Johansson, V. Gogvadze, L. Xiao, J. Li, T. Burks, et al. 2012. "Microsomal Glutathione Transferase 1 Protects against Toxicity Induced by Silica Nanoparticles but Not by Zinc Oxide Nanoparticles." *ACS Nano* 6 (3): 1925–1938. doi:10.1021/nn2021056.
- Thoolen, B., R. R. Maronpot, T. Harada, A. Nyska, C. Rousseaux, T. Nolte, D. E. Malarkey, et al. 2010. "Proliferative and Nonproliferative Lesions of the Rat and Mouse Hepatobiliary System." *Toxicologic Pathology* 38 (7): 55–81S. doi:10.1177/0192623310386499.
- Vogel, U., and F. R. Cassee. 2018. "Editorial: Dose-Dependent ZnO Particle-Induced Acute Phase Response in Humans Warrants Re-Evaluation of Occupational Exposure Limits for Metal Oxides." *Particle and Fibre Toxicology* 15 (1): 7. doi:10.1186/s12989-018-0247-3.
- Warheit, D. B., C. M. Sayes, and K. L. Reed. 2009. "Nanoscale and Fine Zinc Oxide Particles: Can in Vitro Assays Accurately Forecast Lung Hazards following Inhalation Exposures?" *Environmental Science & Technology* 43 (20): 7939–7945. doi:10.1021/es901453p.
- Wohlleben, W., S. Brill, M. W. Meier, M. Mertler, G. Cox, S. Hirth, B. von Vacano, et al. 2011. "On the Lifecycle of Nanocomposites: Comparing Released Fragments and Their in-Vivo Hazards from Three Release Mechanisms and Four Nanocomposites." *Small (Weinheim an Der Bergstrasse, Germany)* 7 (16): 2384–2395. doi:10.1002/sml.201002054.
- Xu, J., H. Shi, M. Ruth, H. Yu, L. Lazar, B. Zou, C. Yang, A. Wu, and J. Zhao. 2013. "Acute Toxicity of Intravenously Administered Titanium Dioxide Nanoparticles in Mice." *PLoS One* 8 (8): e70618. doi:10.1371/journal.pone.0070618.